Medicinal Chemistry Research (2021) 30:685–701
https://doi.org/10.1007/s00044-020-02670-w

MEDICINAL CHEMISTRY RESEARCH

ORIGINAL RESEARCH

Molecular hybridization based design and synthesis of new *benzo[5,6]chromeno[2,3-b]-quinolin-13(14H)-one* analogs as cholinesterase inhibitors

Baswaraju Macha[1] · Ravindra Kulkarni[2] · Chandrakant Bagul[2] · Anil Kumar Garige[3] · Raghuramrao Akkinepally[1] · Achaiah Garlapati[1]

Received: 7 August 2020 / Accepted: 16 November 2020 / Published online: 8 January 2021

Abstract

A Series of new tacrine analogs were designed, synthesized, characterized by respective spectral data and evaluated for cholinesterase inhibitory activity to be useful in Alzheimer's disease. Most of the synthesized compounds showed good in vitro inhibitory activities toward acetyl cholinesterase (AChE) and butyrylcholinesterase (BuChE) enzymes. Among the compounds, **6i, 6o and 6r** with increased saturated carboxylic ring size attached to the pyridine moiety and having 3,4-dihydroxy, 3,4,5-trimethoxy substituents on the aromatic ring attached at the stereogenic center have shown equal potency to that of tacrine with IC_{50}values 0.65 ± 0.06, 1.32 ± 0.02 and 0.85 ± 0.05, 1.65 ± 0.12 and 0.92 ± 0.03, 1.91 ± 0.12 μM against AChE and BuChE, respectively. Standard drug tacrine exhibited IC_{50} values of 0.47 ± 0.02 and 0.65 ± 0.08, while Donepezil showed IC_{50} 0.71 ± 0.06 and 0.31 ± 0.04 μM against AChE and BuChE, respectively. Docking studies of all the molecules disclosed close hydrogen bond interactions with the binding site.

Keywords Alzheimer's disease · Antioxidants · Anti-inflammatory · Cholinesterase inhibitor · Multi targeted ligands

Introduction

Alzheimer's disease (AD) is also discerned as senile dementia of the Alzheimer's type (SDAT), a form of brain disease, affecting a large population of geriatric patients. It is a progressive neurodegenerative disease involving early decline in memory associated with the other symptoms such as disturbances in language, visuospatial abnormalities and loss of cognition which aggrandize to severe with time and ultimately death. AD is now the fourth leading reason for human mortality in the western countries following cardiovascular disease, cancer, and cerebrovascular disease [1]. World health organization (WHO) has conjectured that in the next century, AD will be more widespread than AIDS, cancer and cardiovascular diseases [2]. In USA, over 17% of people with age above 75 suffer with AD with an estimated cost of whooping USD 236 billion for the treatment which may escalate over USD 700 billion by 2050 [3]. The etiology of AD has not been explicated yet, however quite a lot of factors including amyloidal-β (Aβ) deposits, tau protein aggregation, exitotoxity hypothesis, oxidative stress [4] and declined acetylcholine levels [5] have been implicated in the pathomechanism of AD. It has also been hypothesized that oxidative damage to the intracellular structures may also decline mitochondrial metabolism which act as causative factor of abnormal cellular function and apparently cell death and initiate inflammatory symptoms [6–8]. Currently no complete treatment is available to cure AD and clinical treatments have only symptomatic effects. Enumerable drugs have already been employed to contain the brain Aβ levels either by decreasing its

Supplementary information The online version of this article (https://doi.org/10.1007/s00044-020-02670-w) contains supplementary material, which is available to authorized users.

✉ Achaiah Garlapati
achaiah_g@yahoo.co.in

[1] Medicinal Chemistry Division, University College of Pharmaceutical Sciences, Kakatiya University, Warangal, Telangana 506009, India

[2] Bharati Vidyapeeth's Poona College of Pharmacy, Paud Road, Erandawane, Pune 411038, India

[3] Jayamukhi Institute of Pharmaceutical Sciences, Narsampet, Warangal 506332, India

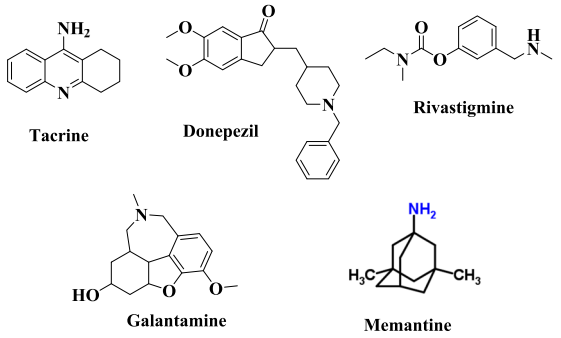

Fig. 1 Structure of anti-Alzheimer's drug

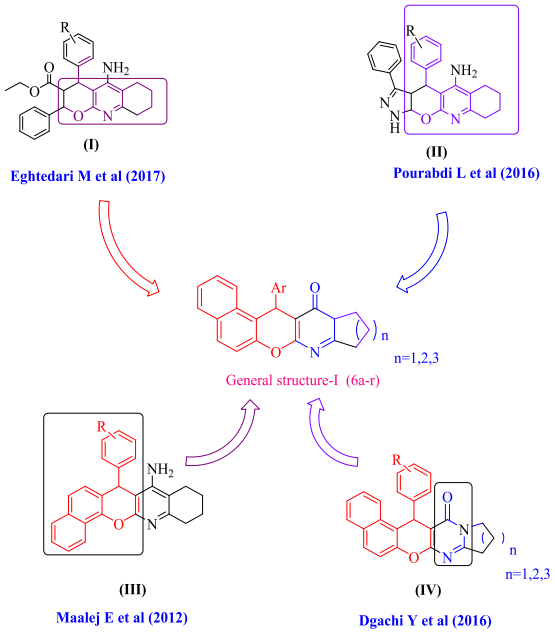

Fig. 2 Design of New *10,11,12,12a-tetrahydro-9H-benzo[5,6]chromeno[2,3-b]quinolin-13(14H)-one* analogs

production or its clearance, however such approach failed to enhance the cognitive ability of AD patients in trials. Latest drug discovery in AD segment targeting BACE (beta-site amyloid precursor protein cleaving enzyme) have failed to live up to the expectations due to associated toxicities. Drugs like tacrine, donepezil, galantamine and rivastigmine which act by elevating acetylcholine (ACh) levels by inhibiting acetylcholinesterase (AChE) and memantine, a NMDA receptor antagonist (Fig. 1). The first clinical candidate to be introduced in the market for treatment of AD was tacrine and has been discontinued from the therapy due to its severe hepatotoxicity which is attributed to the free primary amine group.

Aforementioned AChEIs have demonstrated a great success in raising ACh levels in brain by decreasing the activity of AChE in the specific regions of the brain. This elevated levels of ACh was short lived and brain biochemical analysis of AD patients have revealed that it was due to uninterrupted BuChE activity despite reduced AChE level. The drug discovery in AD is gradually drifting from "one target, one disease" to "multi-target-directed ligands" (MTDLs) [9], which are capable of simultaneously inhibiting both AChE and BuChE [10–12]. Having understood to some extent the pathogenesis of AD, it is palpable thought that multi-targeting with single drug could eventually control the AD. The multi-targeting could involve inhibiting ChE and free radicals or AChE and BuChE in single shot. Replacement or annulating the benzene ring in tacrine with different heterocyclic rings was considered as important in design of tacrine like compounds. Eghtedari et al. [13] reported a series of poly functionalized tacrine derived compounds, *5-amino-2-phenyl-4H-pyrano [2,3-b] quinoline-3-carboxylate* **(I)** as potent inhibition of cholinesterases. The most potent compound with *4-(3-bromophenyl)* moiety exhibited IC_{50} values of 0.069 and 1.35 µM, respectively, against AChE and BuChE. A series of tacrine-based pyrano[2,3-*c*] pyrazoles **(II)** were reported as potent inhibitors of cholinesterases. A few of them showed IC_{50} values in the nanomolar level [14].

Maalej et al. [15] synthesized a number of racemic tacrine analogs containing*7-aryl-9,10,11,12-tetrahydro-7H-benzo[7,8]chromeno[2,3-b]quinoline-8-amine* structure **(III)** as potential candidates for the treatment of Alzheimer's disease, with potent antioxidant and anticholinesterse activities. Dgachi et al. [16] designed new benzochromenopyrimidinones **(IV)**. Among the series, compounds with a piperdine-fused ring ($n = 2$) and 4-methyl/ methoxy substituents on phenyl ring were found to be potent AChEIs. In the present study, we used molecular hybridization to design *benzo[5,6]chromenopyridinones* (**6a-r**) as depicted in Fig. 2 and report the synthesis and AChE and BuChE inhibitory activity to be useful as anti-Alzheimer's agents.

Materials and methods

Chemistry

All chemicals including standard drugs and solvents were procured from Sigma-Aldrich, HiMedia, Bangalore, India and others and were used without further purification with the exception of liquid aldehydes which were purified by using standard procedures prior to use. Melting point for all the compounds was recorded in open capillary tubes using VEEGO VMP-D Digital melting point apparatus. FTIR spectra were done on JASCO FTIR 4100 series by using KBr pellets and are reported in cm^{-1}. Signals of ^{1}H NMR and ^{13}C NMR spectra were measured on a BRUKER-II 400 (400 MHz NMR, ^{13}C NMR 100 MHz) spectrophotometer

by taking TMS as internal standard. Pre-coated TLC plates were used to check the purity of the compounds and spots were visualized by using iodine vapors and ultra-violet rays. Elemental analyses were carried out by a CHN-Vario Elico Micro elemental analyzer. The estimation of biochemical parameters was carried out using commercially available test kits (Sigma-Aldrich).

General procedure for synthesis of ethyl aminobenzochromene-2-carboxylates (4a-f)

A mixture of 2-naphthol (**1**, 10 mmol), aromatic aldehyde (**2a-f**, 10 mmol) and ethyl cyanoacetate (**3**, 10 mmol) were refluxed in ethanol for 10 h with stirring in the presence of piperidine (0.2 eq.). The crude precipitate resulted in was filtered, washed with cold ethanol and dried to produce the desired compounds (**4a-f**).

General procedure for the synthesis of benzochromeno*[5,6]* pyridinones (6a-r)

Phosphorous oxychloride (0.14 mL, 0.23 g, 1.5 eq.) was dropped in portion to the solution of the appropriate ethyl amino benzochromene-2-carboxylates(**4a-f)** and the appropriate cycloalkanones (**5a-c**, $n = 1$, 2, 3: 1.5 eq.) in 1,2-dichloroethane. The mixture was refluxed for 10 h with stirring and maximum part of solvent was evaporated and water (10 mL) was added. The solution was basified with 20% aqueous NaOH, and extracted with DCM, the organic layer washed with water and dried over magnesium sulfate. The organic volatilities were evaporated, the solid obtained was washed with ether and filtered to give benzochromenopyridinones (**6a-r**).

Characterization of compounds

13-Phenyl-9, 10, 11, 11a-tetrahydrobenzo *[5,6]*chromeno [2,3-*b*]cyclopenta[e] pyridin-12(13*H*)-one (6a)

Compound **6a** obtained as yellowish orange solid (yield 27%), m. p. 165–167 °C. ^{1}H NMR (400 MHz DMSO, δ ppm): 8.09–8.11 (d, 1H, $J = 8.0$ Hz, Ar–H), 7.81–7.82 (d, 1H, $J = 4.0$ Hz, Ar–H) 7.55–7.56 (d, 1H, $J = 4.0$ Hz, Ar–H), 7.51–7.53 (t, 1H, $J = 4.0$ Hz Ar–H), 7.35–7.39 (t, 1H, $J = 8.0$ Hz Ar–H), 7.23–7.33 (m,7H, Ar–H), 5.351 (s, 1H), 3.18–3.21 (t, 1H, $J = 8.0$ Hz), 2.71–2.76 (m, 2H), 1.90–2.02 (m, 2H), 1.72–1.88 (m, 6H); ^{13}C NMR (100 MHz, DMSO): 191.15, 160.25, 158.15, 154.17, 145.12, 135.18, 130.25, 128.10, 127.38, 127.84 126.24, 125.18, 125.01, 124.25, 116.52, 101.28, 60.21, 57.40, 48.58, 38.04, 29.29. MASS spectrum m/z: 366.14 $[M + H]^+$ Calc. for $C_{25}H_{19}NO_2$; CHN: C, 82.17; H, 5.24; N, 3.83; O, 8.76; Found: C, 82.05; H, 5.10; N, 3.78; O, 8.70. IR (KBr, cm^{-1}): 3060.21 (C–H, Aromatic), 2968.10 (C–H, Aliphatic), 1716.96 (C = O), 1516.01 (C = C, Aromatic), 1265.51 (C–O).

14-Phenyl-10, 11, 12, 12a-tetrahydro-9*H*-benzo *[5,6]* chromeno [2,3-*b*]quinolin-13 (14*H*)-one (6b)

Compound **6b** obtained as yellowish white solid (yield 30%), m. p. 201–203 °C. ^{1}H NMR (400 MHz DMSO, δ ppm): 8.09–8.11 (d, 1H, $J = 8.0$ Hz, Ar–H), 7.80–7.82 (d, 1H, $J = 8.0$ Hz, Ar–H), 7.76–7.78 (d, 1H, $J = 4.0$ Hz, Ar–H), 7.50–7.53 (t, 1H, $J = 4.0$ Hz, Ar–H), 7.37–7.39 (t, 1H, $J = 4.0$ Hz, Ar–H), 7.32–7.36 (m, 4H, Ar–H), 7.23–7.31 (m, 2H, Ar–H), 5.351 (s, 1H), 3.19–3.21 (t, 1H, $J = 4.0$ Hz), 2.71–2.76 (m, 2H), 1.90–2.02 (m, 4H), 1.72–1.88 (m, 6H). ^{13}C NMR (100 MHz, DMSO): 191.15, 160.25, 158.15, 154.17, 145.12, 135.18, 130.25, 128.10, 127.38, 127.84 126.24, 125.18, 125.01, 124.25, 116.52, 101.28, 60.21, 57.40, 48.58, 38.04, 29.29. MASS spectrum m/z: 380.20 $[M + H]^+$ Calc. for $C_{26}H_{21}NO_2$; CHN: C, 82.30; H, 5.58; N, 3.69; O, 8.43; Found: C, 82.36; H, 5.62; N, 3.65; O, 8.40. IR (KBr, cm^{-1}): 3103.33 (C–H, Aromatic), 2922.15 (C–H, Aliphatic), 1718.28 (C = O), 1590.56 (C = C, Aromatic), 1184.54 (C–O).

15-Phenyl-9,10,11,12,13,13a-hexahydrobenzo [5,6] chromeno [2,3-*b*] cyclohepta [*e*] pyridin-14 (15*H*)-one (6c)

Compound **6c** obtained as white solid (yield 39%), m. p. 181–191 °C. ^{1}H NMR (400 MHz $CDCl_3$, δ ppm): 7.91–7.93 (d, 2H, $J = 8.0$ Hz, Ar–H), 7.71–7.73 (t, 1H, $J = 4.0$ Hz, Ar–H) 7.71–7.73 (t, 1H, $J = 4.0$ Hz, Ar–H), 7.47–7.56 (m, 3H, Ar–H), 7.35–7.39 (t, 2H, Ar–H), 7.18–7.20 (d, 2H, Ar–H), 5.53 (s, 1H), 1.69–1.71 (t, 2H, $J = 4.0$ Hz), 1.36–1.45 (m, 2H), 1.10–1.33 (m, 2H), 0.92–0.95 (m, 4H). ^{13}C NMR (100 MHz, $CDCl_3$): 193.09, 165.36, 160.20, 156.25, 145.12, 134.10, 131.10, 128.32, 128.04, 127.12, 126.58, 125.10, 125.51 123.24, 113.15, 105.10, 68.15, 58.17, 45.14, 36.14, 20.14; MASS spectrum m/z: 394.18 $[M + H]^+$ Calc. for $C_{27}H_{23}NO_2$; CHN: C, 82.42; H, 5.89; N, 3.56; O, 8.13; Found: C, 82.40; H, 5.84; N, 3.52; O, 8.10. IR (KBr, cm^{-1}): 3058.56 (C–H, Aromatic), 2976.58 (C–H, Aliphatic), 1724.84 (C = O), 1591.59 (C = C, Aromatic), 1080.34 (C–O).

13-(Naphthalen-2-yl)-9,10,11,11a-tetrahydrobenzo[5,6] chromeno[2,3-*b*]cyclopenta [e] pyridin-12(13*H*)-one (6d)

Compound **6d** obtained as orange solid (yield 26%), m. p. 158–160 °C. ^{1}H NMR (400 MHz $CDCl_3$, δ ppm): 8.49–8.51 (d, 1H, $J = 8.0$ Hz, Ar–H), 7.95–8.00 (t, 1H, $J = 10$ Hz, Ar–H) 7.89–7.91 (d, 1H, $J = 8.0$ Hz, Ar–H), 7.77–7.81 (t, 2H, $J = 8.0$ Hz, Ar–H), 7.63–7.67 (m, 2H,

Ar–H), 7.38–7.47 (m, 2H, Ar–H), 7.19–7.23 (t, 1H, J = 8.0 Hz, Ar–H), 6.80–6.82 (d, 1H, J = 9.6 Hz, Ar–H), 6.267 (s, 1H, Ar—H), 5.418 (s, 1H), 1.33–1.44 (m, 4H), 1.10–1.127 (m, 3H), 0.91–0.95 (m, 2H). ^{13}C NMR (100 MHz, $CDCl_3$): 193.09, 165.36, 160.20, 156.25, 145.12, 134.10, 131.10, 128.32, 128.04, 127.12, 126.58, 125.10, 125.51 123.24, 113.15, 105.10, 68.15, 58.17, 45.14, 36.14, 20.14; Mass spectrum m/z: 416.16 $[M + H]^+$ Calc. for $C_{29}H_{21}NO_2$; CHN: C, 83.83; H, 5.09; N, 3.37; O, 7.70; Found: C, 83.80; H, 5.14; N, 3.32; O, 7.75. IR (KBr, cm^{-1}): 3071.66 (C–H, Aromatic), 2981.22 (C–H, Aliphatic), 1730.51 (C = O), 1591.45 (C = C Aromatic), 1294.70 (C–O).

14-(Naphthalen-2-yl)-10,11,12,12a-tetrahdro-9H-benzo[5,6] chromeno[2,3-b]-Quinolin-13(14H)-one (6e)

Compound 6e obtained as orange solid (yield 51%), m. p. 196-198 °C. ^{1}H NMR (400 MHz $CDCl_3$, δ ppm): 8.49–8.51 (d, 1H, J = 8.0 Hz, Ar–H), 7.95–8.00 (t, 2H, J = 8.4 Hz, Ar–H), 7.89–7.91 (d, 1H, J = 8.0 Hz, Ar–H), 7.77–7.81 (t, 1H, J = 6.0 Hz, Ar–H), 7.63–7.68 (m, 3H, Ar–H), 7.40–7.47 (m, 3H, J = 8.0 Hz, Ar–H), 7.19–7.23 (t, 1H, J = 7.6 Hz, Ar–H), 6.81–6.83 (d, 1H, J = 7.2 Hz, Ar–H), 4.30 (s, 1H), 1.30–1.49 (m, 6H), 1.11–1.15(t, 3H, J = 6.0 Hz). ^{13}C NMR (100 MHz, $CDCl_3$): 196.34, 168.13, 164.53, 153.78, 152.34, 143.63, 142.44, 139.59, 138.74, 136.03, 129.96, 129.40, 127.96, 127.65, 126.73, 125.01, 119.69, 48.15, 38.66, 32.03, 26.21, 22.30. MASS spectrum m/z: 430.52 $[M + H]^+$ Calc. for $C_{26}H_{20}N_2O_4$; CHN: C, 73.57; H, 4.75; N, 6.60; O, 15.08; Found: C, 73.53; H, 4.70; N, 6.65; O, 15.09. IR (KBr, cm^{-1}): 3086.15 (C–H, Aromatic), 2922.18 (C–H, Aliphatic), 1722.81 (C = O), 1549.75 (C = C, Aromatic), 1210.31 (C–O).

15-(Naphthalen-2-yl)-9,10,11,12,13,13a-hexahydrobenzo [5,6] chromeno[2,3-*b*] cyclohepta [e] pyridin-14(15*H*)-one (6 f)

Compound **6 f** obtained as orange solid (yield 49%), m. p.210–212 °C. ^{1}H NMR (400 MHz $CDCl_3$, δ ppm): 8.49–8.51 (d, 1H, J = 8.0 Hz, Ar–H), 7.95–8.00 (t, 2H, J = 8.4 Hz, Ar–H) 7.89–7.91 (d, 1H, J = 8.0 Hz, Ar–H), 7.77–7.81 (t, 2H, J = 6.0 Hz Ar–H), 7.63–7.67 (m, 2H, Ar–H), 7.28–7.47 (m, 3H, Ar–H), 7.19–7.23 (t, 1H, J = 7.6 Hz, Ar–H), 6.80–6.82 (d, 1H, J = 7.2 Hz, Ar–H), 6.27 (s, 1H, Ar–H), 4.29 (s, 1H), 1.41–1.51 (m, 6H), 1.11–1.14 (t, 5H, J = 7.2 Hz). ^{13}C NMR (100 MHz, $CDCl_3$): 196.6, 164.6, 161.3, 152.3, 138.4, 137.2, 135.2, 133.7, 132.9, 131.8, 129.9, 128.0, 127.6, 127.5, 127.4, 127.3, 127.0, 126.5,126.0, 125.1, 120.2, 117.6, 116.1, 109.3, 52.7, 38.9, 38.3, 23.7, 14.9; MASS spectrum m/z: 444.58 $[M + H]^+$ Calc. for $C_{31}H_{25}NO_2$; CHN: C, 83.95; H, 5.68; N, 3.16; O, 7.21; Found: C, 83.92; H, 5.72; N, 3.20; O, 7.25. IR (KBr, cm^{-1}): 3067.12 (C–H, Aromatic), 2938.02 (C–H, Aliphatic), 1720.32 (C = O), 1515.12 (C = C, Aromatic), 1124.61 (C–O).

13-(3-Chlorophenyl)-9,10,11,11a-tetrahydrobenzo[5,6] chromeno [2,3-*b*] cyclopenta [*e*]pyridin-12(13*H*)-one (6 g)

Compound **6 g** obtained as yellow solid (yield 48%), m. p.186–188 °C. ^{1}H NMR (400 MHz $CDCl_3$, δ ppm): 8.09–8.11 (d, 1H, J = 8.0 Hz, Ar–H), 7.80–7.81 (d, 1H, J = 4.0 Hz, Ar–H), 7.76–7.77 (d, 1H, J = 4.0 Hz, Ar–H), 7.50–7.53 (t, 2H, J = 6.0 Hz, Ar–H), 7.17–7.39 (m, 3H, Ar–H), 7.13–7.14 (d, 1H, J = 4.0 Hz, Ar–H), 7.11–7.12 (d, 1H, J = 4.0 Hz, Ar–H), 5.31 (s, 1H), 3.18–3.21 (t, 1H, J = 4.0 Hz), 2.67–2.74 (m, 2H,), 1.72–1.88 (m, 4H). ^{13}C NMR (100 MHz, $CDCl_3$):196.10, 160.25, 158.15, 154.17, 145.12, 135.18, 130.25, 128.10, 128.02, 127.38, 127.84 126.24, 126.10, 125.18, 125.01, 124.25, 116.52, 101.28, 60.21, 57.40, 48.58, 38.04, 29.29, 14.09; MASS spectrum m/z: 403.24 $[M + H]^+$ Calc. for $C_{25}H_{18}ClNO_2$: CHN: C, 75.09; H, 4.54; N, 3.50; O, 8.00; Found: C, 75.15; H, 4.50; N, 3.59; O, 8.04. IR (KBr, cm^{-1}): 3068.23 (C–H, Aromatic), 2980.18 (C–H, Aliphatic), 1720.13 (C = O), 1516.04 (C = C, Aromatic), 1124.61 (C–O).

14-(3-Chlorophenyl)-10,11,12,12a-tetrahydro-9H-benzo [5,6] chromeno [2,3-*b*] quinolin-13(14*H*)-one (6 h)

Compound **6 h** obtained as cream solid (yield 38%), m. p.163–165 °C. ^{1}H NMR (400 MHz DMSO, δ ppm): 8.09–8.11(d, 1H, J = 8.0 Hz, Ar–H), 7.80–7.82 (d, 1H, J = 8.0 Hz, Ar–H), 7.76–7.77 (d, 1H, J = 4.0 Hz, Ar–H), 7.50–7.52 (t, 2H, J = 4.2 Hz, Ar–H), 7.29–7.38 (m, 3H, Ar–H), 7.25–7.26 (d, 1H, J = 4.0 Hz, Ar–H), 5.30 (s, 1H), 3.26–3.28 (t, 1H, J = 4.0 Hz), 3.07–3.11 (m, 2H), 1.82–1.84 (t, 1H, J = 4.2 Hz), 1.70–1.76 (m, 2H). ^{13}C NMR (100 MHz, DMSO): 196.10, 160.25, 158.15, 154.17, 145.12, 135.18, 130.25, 128.10, 128.02, 127.38, 127.84 126.24, 126.10, 125.18, 125.01, 124.25, 116.52, 101.28, 60.21, 57.40, 48.58, 40.12 38.04, 29.29, 14.09; MASS spectrum m/z: 415.10 $[M + H]^+$ Calc. for $C_{26}H_{20}ClNO_2$; CHN: C, 75.45; H, 4.87; N, 3.38; O, 7.73; Found: C, 75.40; H, 4.89; N, 3.32; O, 7.75. IR (KBr, cm^{-1}): 3089.23 (C–H, Aromatic), 2965.18 (C–H, Aliphatic), 1715.10 (C = O), 1535.14 (C = C, Aromatic), 1140.12 (C–O).

15-(3-Chlorophenyl)-9,10,11,12,13,13a-hexahydrobenzo [5,6] chromeno[2,3-*b*] cyclohepta [e] pyridin-14 (15*H*)-one (6i)

Compound **6i** obtained as light yellow solid (yield 45%), m. p.190–192 °C. ^{1}H NMR (400 MHz DMSO, δ ppm):

8.10–8.12 (d, 1H, $J = 8.0$ Hz, Ar–H), 7.81–7.82 (d, 1H, $J =$ 4.0 Hz, Ar–H), 7.76–7.78 (d, 1H, $J = 8.0$ Hz, Ar–H), 7.50–7.54 (t, 2H, $J = 8.0$ Hz, Ar–H), 7.20–7.34 (m, 3H, Ar–H), 7.14–7.16 (d, 1H, $J = 8.0$ Hz, Ar–H), 7.11–7.13 (d, 1H, $J = 8.0$ Hz, Ar–H), 5.34 (s, 1H), 3.21–3.24 (t, 3H, $J =$ 6.8 Hz), 2.67–2.74 (m, 4H,), 1.72–1.88 (m, 4H). ^{13}C NMR (100 MHz, DMSO): 196.06, 164.06, 161.03, 151.08, 141.07, 134.80, 133.51, 130.16, 128.28, 128.15, 128.10, 128.04, 126.32, 126.12, 126.04, 123.08, 123.02, 122.10, 118.09, 109.3, 47.05, 35.30, 34.17, 28.21, 27.50, 26.14, 22.30. MASS spectrum m/z: 429.32 $[M + H]^+$ Calc. for $C_{27}H_{22}ClNO_2$; CHN: C, 75.78; H, 5.18; N, 3.27; O, 7.48; Found: C, 75.70; H, 5.21; N, 3.29; O, 7.41. IR (KBr, cm^{-1}): 3071.13(C–H, Aromatic), 2957.18 (C–H Aliphatic), 1718.10 (C = O), 1524.12(C = C, Aromatic), 1132.14 (C–O).

13-(3-Nitrophenyl)-9,10,11,11a-tetrahydrobenzo[5,6] chromeno[2,3-*b*]cyclopenta [e] pyridin-12(13*H*)-one (6j)

Compound **6j** obtained as light orange solid (yield 21%), m. p. 186–188 °C. ^{1}H NMR (400 MHz $CDCl_3$, δ ppm): 8.12 (s, 1H, Ar–H), 8.04–8.06 (d, 1H, $J = 8.0$ Hz, Ar–H), 7.80–7.82 (d, 1H, $J = 8.0$ Hz, Ar–H), 7.70–7.72 (d, 1H, $J = 8.0$ Hz, Ar–H), 7.40–7.43 (t, 1H, $J = 4.2$ Hz, Ar–H), 7.29–7.31 (t, 1H, $J = 6.8$ Hz, Ar–H), 7.26–7.28 (d, 1H, $J = 8.0$ Hz, Ar–H), 6.70–6.71 (d, 1H, $J = 4.0$ Hz, Ar–H), 6.62–6.64 (d, 1H, $J = 6.8$ Hz, Ar–H), 5.35 (s, 1H), 3.18–3.21 (t, 3H, $J =$ 4.0 Hz), 2.72–2.78 (m, 6H), 1.74–1.96 (m, 6H); ^{13}C NMR (100 MHz, $CDCl_3$): 196.6, 164.6, 161.03, 152.06, 151.8, 148.04, 133.05, 132.5, 128.8, 128.3, 126.03, 123.08, 123.02, 122.04, 122.01, 119.04, 118.24, 109.03, 52.07, 38.09, 34.21, 23.25, 14.31; MASS spectrum m/z: 411.48 $[M + H]^+$ Calc. for $C_{25}H_{18}N_2O_4$; CHN: C, 73.16; H, 4.42; N, 6.83; O, 15.59; Found: C, 73.20; H, 4.45; N, 6.86; O, 15.62. IR (KBr, cm^{-1}): 3071.05(C–H, Aromatic), 2988.18 (C–H, Aliphatic), 1720.14 (C = O), 1545.38 (C = C, Aromatic), 1148.20 (C–O).

14-(3-Nitrophenyl)-10,11,12,12a-tetrahydro-9H-benzo [5,6] chromeno [2,3-*b*] quinolin-13 (14*H*)-one (6k);

Compound **6k** obtained as white solid (yield 40%), m. p. 190–192 °C. ^{1}H NMR (400 MHz DMSO, δ ppm): 8.14 (s, 1H, Ar–H), 8.06–8.07 (d, 1H, $J = 4.0$ Hz, Ar–H), 7.85–7.87 (d, 1H, $J = 8.0$ Hz, Ar–H), 7.78–7.79 (d, 1H, $J = 8.0$ Hz, Ar–H), 7.41–7.44 (t, 1H, $J = 12.0$ Hz, Ar–H), 7.31–7.33 (t, 1H, $J = 4.0$ Hz, Ar–H), 7.28–7.30 (d, 1H, $J = 8.0$ Hz, Ar–H), 6.78–6.80 (d, 1H, $J = 8.0$ Hz, Ar–H), 6.62–6.63 (d, 1H, $J = 8.0$ Hz, Ar–H), 5.35 (s, 1H), 3.18–3.21 (t, 3H, $J =$ 8.0 Hz), 2.72–2.78 (m, 6H), 1.74–1.96 (m, 8H); ^{13}C NMR (100 MHz, DMSO): 196.6, 164.6, 161.03, 152.06, 151.8, 148.04, 133.05, 132.5, 128.8, 128.3, 126.03, 123.08, 123.02, 122.04, 122.01, 119.04, 118.24, 109.03, 52.07, 45.32, 40.51, 38.09, 34.21, 23.25, 14.31. MASS spectrum m/z: 425.17 $[M + H]^+$ Calc. for $C_{26}H_{20}N_2O_4$; CHN: C, 73.57; H, 4.75; N, 6.60; O, 15.08; Found: C, 73.52; H, 4.80; N, 6.55; O, 15.10. IR (KBr, cm^{-1}): 3068.23 (C–H, Aromatic), 2980.18 (C–H, Aliphatic), 1718.13 (C = O), 1525.04 (C = C, Aromatic), 1135.61 (C–O).

15-(3-Nitrophenyl)-9,10,11,12,13,13a-hexahydrobenzo [5,6] chromeno[2,3-*b*] cyclohepta [e] pyridine-14 (15*H*)-one (6 l)

Compound **6 l** obtained as white solid (yield 36%), m. p. 160–162 °C. ^{1}H NMR (400 MHz, $CDCl_3$, δ ppm): 8.14 (s, 1H, Ar–H), 8.02–8.04 (d, 1H, $J = 8.0$ Hz, Ar–H), 7.87–7.88 (d, 1H, $J = 4.0$ Hz, Ar–H), 7.76–7.78 (d, 1H, J = 8.0 Hz, Ar–H), 7.46–7.48 (t, 1H, $J = 4.0$ Hz, Ar–H), 7.34–7.36 (t, 1H, $J = 4.2$ Hz, Ar–H), 7.30–7.32 (d, 1H, $J = 8.0$ Hz, Ar–H), 6.80–6.82 (d, 1H, $J = 8.0$ Hz, Ar–H), 6.64–6.66 (d, 1H, $J = 8.0$ Hz, Ar–H), 5.35 (s, 1H), 3.18–3.21 (t, $J =$ 4.2 Hz, 3H), 2.72–2.78 (m, 6H), 1.74–1.96 (m, 8H); ^{13}C NMR (100 MHz, $CDCl_3$): 196.6, 164.6, 161.03, 152.06, 151.8, 148.04, 133.05, 132.5, 128.8, 128.3, 126.03, 123.08, 123.02, 122.04, 122.01, 119.04, 118.24, 109.03, 74.21, 68.12 52.07, 45.32, 40.51 38.09, 34.21, 23.25, 14.31; MASS spectrum m/z: 439.28 $[M + H]^+$ Calc. for $C_{27}H_{22}N_2O_4$; CHN: C, 73.96; H, 5.06; N, 6.39; O, 14.60; Found: C, 73.90; H, 5.08; N, 6.40; O, 14.58. IR (KBr, cm^{-1}): 3071.13 (C–H, Aromatic), 2957.18 (C–H Aliphatic), 1718.10 (C = O), 1524.12 (C = C, Aromatic), 1132.14 (C–O).

13-(3,4-Dihydroxyphenyl)-9,10,11,11a-tetrahydrobenzo [5,6] chromeno [2,3-*b*] cyclopenta [e]pyridin-12 (13*H*)-one (6 m)

Compound **6 m** obtained as white solid (yield 48%), m. p. 148–150 °C. ^{1}H NMR (400 MHz DMSO, δ ppm): 8.09–8.11 (d, 1H, J = 8.0 Hz, Ar–H), 7.80–7.82 (d, 1H, J = 8.0 Hz, Ar–H), 7.75–7.77 (d, 1H, J = 8.0 Hz, Ar–H), 7.49–7.53 (t, 1H, J = 8.2 Hz, Ar–H), 7.35–7.39 (t, 1H, J = 12.0 Hz, Ar–H), 7.25–7.26 (d, 1H, J = 8.0 Hz, Ar–H), 6.75–6.77 (d, 1H, Ar–H), 6.67 (s, 1H, Ar–H), 6.65–6.66 (d, 1H, J = 4.0 Hz, Ar–H), 5.34 (s, 1H), 3.18–3.21 (t, 3H, J = 4.0 Hz), 2.70–2.76 (m, 4H), 1.74–1.96 (m, 4H). ^{13}C NMR (100 MHz, DMSO): 196.6, 164.6, 161.3, 151.8, 147.6, 133.5, 129.8, 129.4, 128.6, 128.4, 128.2, 126.3, 126.2, 123.8, 123.8, 123.2, 122.1, 118.9, 109.3, 52.7, 38.6, 35.8, 23.7, 14.9; MASS spectrum peak m/z: 366.32$[M + H]^+$ Calc. for $C_{25}H_{19}NO_4$; CHN: C, 75.55; H, 4.82; N, 3.52; O, 16.10; Found: C, 75.58; H, 4.86; N, 3.50; O, 16.08. IR (KBr, cm^{-1}): 3604.23 (OH), 3067.12 (C–H, Aromatic), 2985.42 (C–H, Aliphatic), 1713.75 (C = O), 1523.20 (C = C, Aromatic), 1268.31(C–O).

14-(3,4-Dihydroxyphenyl)-10,11,12,12a-tetrahydro-9H-benzo[5,6]chromeno[2,3-*b*]quinolin-13 (14*H*)-one (6n)

Compound **6n** obtained as orange solid (yield 35%), m. p. 157–159 °C. ^{1}H NMR (400 MHz DMSO, δ ppm): 8.10–8.12 (d, 1H, J = 8.0 Hz, Ar–H), 7.82–7.84 (d, 1H, J = 8.0 Hz, Ar–H), 7.72–7.73 (d, 1H, J = 4.2 Hz, Ar–H), 7.48–7.51 (t, 1H, J = 4.0 Hz, Ar–H), 7.30–7.33 (t, 1H, J = 4.0 Hz, Ar–H), 7.27–7.29 (d, 1H, J = 8.0 Hz, Ar–H), 6.72–6.74 (d, 1H, J = 8.0 Hz, Ar–H), 6.69 (s, 1H, Ar–H), 6.62–6.64 (d, 1H, J = 8.0 Hz, Ar–H), 5.30 (s, 1H), 3.19–3.22 (t, 3H, J = 4.0 Hz,), 2.70–2.76 (m, 4H), 1.74–1.96 (m, 6H). ^{13}C NMR (100 MHz, DMSO): 195.6, 168.6, 163.3, 156.8, 148.2, 132.5, 129.6, 129.3, 128.2, 128.1, 128.0, 126.8, 126.4, 123.8, 123.2, 123.1, 122.8, 118.6, 109.4, 52.1, 38.4, 35.6, 32.8, 30.5, 23.1, 14.9; MASS spectrum m/z: 412.28 $[M + H]^+$ Calc. for $C_{26}H_{21}NO_4$; CHN: C, 75.90; H, 5.14; N, 3.40; O, 15.55; Found C, 75.84; H, 5.18; N, 3.45; O, 15.60. IR (KBr, cm^{-1}): 3082.10 (C–H, Aromatic), 2975.15 (C–H, Aliphatic), 1720.12(C = O), 1541.20 (C = C, Aromatic), 1150.68 (C–O).

15-(3,4-Dihydroxyphenyl)-9,10,11,12,13,13a-hexahydrobenzo [5,6] chromeno [2,3 -*b*] cyclohepta [e] pyridin-14 (15*H*)-one (6o)

Compound **6o** obtained as cream white solid (yield 28%), m. p. 165–167 °C. ^{1}H NMR (400 MHz $CDCl_3$, δ ppm): 8.06–8.08 (d, 1H, J = 8.0 Hz, Ar–H), 7.80–7.82 (d, 1H, J = 8.0 Hz, Ar–H), 7.70–7.72 (d, 1H, J = 8.0 Hz, Ar–H), 7.40–7.43 (t, 1H, J = 4.0 Hz, Ar–H), 7.29–7.31 (t, 1H, J = 4.0 Hz, Ar–H), 7.26–7.28 (d, 1H, J = 8.0 Hz, Ar–H), 6.70–6.72 (d, 1H, J = 8.0 Hz, Ar–H), 6.68 (s, 1H, Ar–H), 6.62–6.64 (d, 1H, J = 8.0 Hz, Ar–H), 5.35 (s, 1H), 3.18–3.21 (t, 3H, J = 4.0 Hz), 2.72–2.78 (m, 6H), 1.74–1.96 (m, 6H). ^{13}C NMR (100 MHz, $CDCl_3$): 196.2, 170.4, 168.1, 158.2, 145.2, 138.2, 129.5, 129.3, 128.2, 128.1, 128.0, 126.8, 126.4, 123.8, 123.2, 123.1, 122.8, 118.6, 109.4, 58.32, 52.1, 41.23, 38.4, 35.6, 32.8, 30.5, 23.1, 14.9; MASS spectrum m/z: 426.48 $[M + H]^+$ Calc. for $C_{27}H_{23}NO_4$; CHN: C, 76.22; H, 5.45; N, 3.29; O, 15.04; Found C, 76.20; H, 5.40; N, 3.32; O, 15.10. IR (KBr, cm^{-1}): 3068.52(C–H, Aromatic), 2980.20 (C–H, Aliphatic), 1716.34(C = O), 1535.12(C = C, Aromatic), 1135.18(C–O).

13-(3,4,5-Trimethoxyphenyl)-9,10,11,11a-tetrahydrobenzo [5,6] chromeno [2,3-*b*]cyclopenta[e] pyridin-12(13*H*)-one (6p)

Compound **6p** obtained as yellowish orange solid (yield 26%), mp 198–200 °C. ^{1}H NMR (400 MHz $CDCl_3$, δ ppm): 7.864–7.917 (m, 3H, Ar–H), 7.531–7.568 (t, J = 7.6 Hz, 1H, Ar–H), 7.469–7.506 (t, J = 6.8 Hz, 1H, Ar–H), 7.373–7.395 (d, J = 8.8 Hz, 2H, Ar–H), 6.377 (s, 2H, Ar–H), 5.351 (s, 1H), 3.797 (s, 3H, OCH_3), 3.750 (s, 6H, OCH_3), 1.106–1.378 (m, 4H), 1.024–1.060 (t, 3H, J = 7.2 Hz). ^{13}C NMR (100 MHz, $CDCl_3$): 192.43, 160.15, 159.31, 153.50, 143.20, 138.10, 134.12, 128.19, 128.12, 127.20, 126.10, 124.15, 123.25, 116.32, 105.18, 61.28, 57.10, 49.10, 38.18, 28.65; MASS spectrum m/z: 456.14 $[M + H]^+$ Calc. for $C_{28}H_{25}NO_5$; CHN: C, 73.83; H, 5.53; N, 3.08; O, 17.56; Found C, 73.80; H, 5.51; N, 3.04; O, 17.54. IR spectrum (KBr, cm^{-1}): 3085.98 (C–H, Aromatic), 2974.62 (C–H, Aliphatic), 1718.40 (C = O), 1585.10 (C = C, Aromatic, 1289.04 (C–O).

14-(3,4,5-Trimethoxyphenyl)-10,11,12,12a-tetrahydro-9H-benzo[5,6]chromeno [2,3-*b*] quinolin-13(14*H*)-one (6q)

Compound **6q** obtained as white solid (yield 34%), m. p. 172–174 °C. ^{1}H NMR (400 MHz $CDCl_3$, δ ppm): 7.867–7.891(d, J = 9.6 Hz, 2H, Ar–H), 7.526–7.563 (t, J = 8.8 Hz, 1H, Ar–H), 7.462–7.499 (t, J = 14.8 Hz, 1H, Ar–H), 7.373–7.395 (d, J = 8.8 Hz, 2H, Ar–H), 6.378 (s, 2H, Ar–H), 5.351 (s, 1H), 3.797 (s, 3H, OCH_3), 3.750 (s, 6H, OCH_3), 1.106–1.378 (m, 6H), 1.024–1.060 (t, 3H, J = 7.2 Hz). ^{13}C NMR (100 MHz, $CDCl_3$): 93.23, 162.58, 158.38, 152.05,141.65, 135.65, 130.25, 129.85, 129.32, 128.16, 126.32, 125.45, 123.12, 117.12, 102.16, 61.28, 58.32, 48.12, 36.78, 29.54, 25.07. MASS spectrum m/z: 470.10 $[M + H]^+$ Calc. for $C_{29}H_{27}NO_5$; CHN: C, 74.18; H, 5.80; N, 2.98; O, 17.04; Found C, 74.10; H, 5.78; N, 2.95; O, 17.01. IR (KBr, cm^{-1}): 3086.15 (C–H, Aromatic), 2922.83 (C–H, Aliphatic), 1722.81 (C = O), 1549.75 (C = C, Aromatic), 1269.79 (C–O).

15-(3,4,5-Trimethoxyphenyl)-9,10,11,12,13,13a-hexahydrobenzo[5,6] chromeno [2,3-*b*] cyclohepta[e] pyridin-14(15*H*)-one (6r)

Compound **6r** obtained as yellow solid (yield 45%), m. p.180–182 °C. ^{1}H NMR (400 MHz $CDCl_3$, δ ppm): 7.865–7.919 (m, 5H, Ar–H), 7.473–7.555 (m,2H, Ar–H), 7.316–7.428 (m, 2H, Ar–H), 6.500 (s, 2H, Ar–H), 5.351 (s, 1H), 3.803 (s, 6H, OCH_3), 3.757 (s, 3H, OCH_3), 1.217–1.431 (m, 6H), 1.035–1.071 (m, 5H); ^{13}C NMR (100 MHz, $CDCl_3$):192.59, 162.14, 157.81, 152.64, 142.08, 132.54, 131.08, 129.35, 129.09, 128.56, 128.24, 125.58, 125.25, 124.18, 116.04, 101.28, 60.21, 57.40, 48.58, 38.04, 36.24, 29.29, 25.07, MASS spectrum m/z: 484 $[M + H]^+$ Calc. for $C_{30}H_{29}NO_5$; CHN: C, 74.52; H, 6.04; N, 2.90; O, 16.54; Found C, 74.50; H, 6.02; N, 2.95; O, 16.50. IR (KBr, cm^{-1}): 3051.89 (C–H, Aromatic), 2922.61 (C–H, Aliphatic), 1722.32 (C = O), 1588.12 (C = C, Aromatic), 1253.72 (C–O).

Pharmacological screening

All the tests were organized and conducted in accordance with the standard guiding principles of the CPCSEA, New Delhi and protocol was approved by Institutional Animal Ethical Committee (IAEC/40/UCPSc/KU/2018). 5–6 Weeks male swiss albino mice weighing 20–25 g were used for behavioral studies and the animals were kept under standard environmental conditions viz., 20–25 °C temperature, 12 h lights/dark cycle and given standard pellet diet and water *ad libitum*. The animals were allowed to acclimatize for a week prior to the testing to the laboratory conditions and randomly divided into five groups of six animals each as described below:

Group 1: (vehicle control): Animals received PBS (Phosphate Buffer Solution), p.o

Group 2: (negative control): Mice administered with β-amyloid peptide by cerebroventricular injection.

Group 3: Mice injected with β-amyloid peptide and rivastigmine (p.o.) 5 mg/kg.

Group 4: Mice injected with β-amyloid peptide and Tacrine (p.o.) 5 mg/kg

Group 5: Mice injected with β-amyloid peptide and treated with 200 mg/kg and 400 mg/kg of test compounds (p.o)

All the groups except 1 were administered with 10 µL containing 10 µg Aβ (25–35) peptide [17] for the induction of neurotoxicity at intra-cerebroventicular injection by identifying bregma point in the skull using stereotaxic apparatus (INCO, India). On the 14th day of β-amyloid peptide administration, test compounds and standard drugs were administered. On the 7th day and 21st day after β-amyloid peptide treatment, behavioral studies and biochemical parameters are studied [18].

In vitro AChE and BuChE inhibitory studies [19]

Investigation of AChE and BuChE was carried out by following standard reported procedure and ready to use kits which provided all reagents were supplied by M/s. Sigma Aldrich. Test compounds were solubilized in DMSO and 1% bovine serum and finally diluted with phosphate buffer. Enzyme solutions were prepared to provide a 2.0 unit/ml and solution of Ellman reagent (5, 5′-dithiobis- 2-nitrobenzoic acid, DTNB) was prepared by solubilizing 2 mg of DTNB in 200 mL of buffer with occasional vortex. Determination of IC_{50} of test compounds in modified Ellman method involves formation of thiocholine by the action of AChE. Thiocholine subsequently reacts with DTNB to develop yellow color and the intensity of color is proportionate to the enzyme activity in the presence of test compounds is measured at 412 nm spectroscopically. The assay mixture consisting of 10 µL AChE, 30 µL DTNB solution was taken in a test tube and mixed with occasional shaking. Solution of appropriate concentration of test compounds and standards were added and incubated for 20 min followed by addition of 30 µL DTNB reagent and 30 µL of substrate acetyl thiocholine iodide. The intensity of yellow color thus developed was measured at 412 nm one minute gap at 37 °C in triplicate. The intensity of yellow color developed in stoichiometric reaction indicates the amount of acetyl thiocholine hydrolyzed in the enzymatic reaction. The relative inhibitions of all the test compounds were measured with respect to the native esterase activity. The aforementioned methodology was carried similarly for BuChE activity using butyrylthiocholine iodide as substrate. Linear regression plot drawn between % inhibition vs log concentration of test compounds on MS Excel determines the IC_{50} of compounds. The results are presented as mean ± standard deviation of the triplicates.

In vivo estimation of brain cholinesterases

The modified Ellman method was further followed to estimate brain AChE and BuChE levels in experimental animals. Rat brain was employed to ascertain the cholinesterase inhibitory activity of test compounds in which animals were sacrificed in order to collect the brain and homogenate was prepared 0.1 M phosphate buffer (pH 8.0). To a test tube containing 2.6 mL of phosphate buffer was added 0.4 mL brain homogenate and contents were mixed thoroughly. 100 µL of DTNB chromophore reagent was transferred into the above solution and swirled for proper mixing along with air bubbling. Absorbance of resultant color developed was measured at 412 nm, when absorbance reaches a stable value, it was recorded as the basal reading. Acetyl thiocholine substrate 20 µL was then transferred into test tube and alternation in absorbance was noted for a period of 10 min at intervals of 2 min and later change in the absorbance per minute was determined.

In vivo behavior pharmacological activities

Jumping avoidance box (conditioned avoidance test) [20–22]

Two equal chambers were created by Plexiglas partition in a box and a gate was provided to have access for the animals into the adjacent compartment through 14 × 17 cm space. The test animals are exposed for 30 s to light which is followed by 10 s sound stimulus and a single low intensity foot shock (0.5 mA) for three seconds in each trial. Each mouse from all the groups received 15 such trials in a day with a gap of 15 s between successive trials repeated for 5 days.

Rectangular maze test [23, 24]

Rectangular Maze test apparatus consist of three interconnected chambers A, B and C where in chamber B constituted the maze which is used to explore memory capacity of test animals. All starved mice were allowed to traverse from chamber A to C passing through B. Chamber C contained reward food for animal which traversed from chamber A to C which is indicated by pilot light. All the test animals were trained daily to collect the reward food and time duration was monitored. The animals were considered as trained where in the time required to complete each maze remains constant for three consecutive days and time to traverse for completion of maze was then recorded for each animal before and after treatment with test compounds and standard drug.

Y-maze test [25, 26]

Special recognition memory of mice can be experimented using two trial recognition Y-maze test which does not need learning rule. Working memory of rodents is recorded by the spontaneous Alternation behavior using Y maze which is made up of black painted wood. Y maze made up of three arms, each arm with dimensions 40 cm long, 12 cm high, 3 cm wide at the bottom and 10 cm wide at the top and converged in an equilateral triangular central area. In the experiment which last for 8 min, a mouse is placed in one arm of Y maze and allowed to move freely throughout maze and arm entries (an entry is said to completed when mouse hind paw completely enters the arm) are recorded visually. In Y maze, Alternation term is defined as successive entries into all the three arms and % Alternation is calculated by following expression.

$$\%\text{alternation} = \{(\text{No. ofalternations})/(\text{Total arm entries} - 2)\} \times 100$$

% Alternation hint about the depth of working memory and higher the % is the greater level of memory of the rodents. All the mice in groups except group 1 were injected with β-amyloid protein (10 µg) the day one and all the group mice were trained over maze. On 7th day maze counts were recorded and 14th day standard drugs tacrine and rivastigmine and test compounds administered. On 21st day, once again the mice were allowed move freely on the maze and entry counts were recorded.

Hepatotoxicity [27, 28]

Male Wistar rats with 200–250 g body weight were employed to estimate the hepatotoxicity and animals are sorted into six groups with five rats in each groups. The group animals were provided with amenable environment in separate polypropylene cages and kept at 25 ± 5 °C under 12 h light/dark cycle. Test animals were provided with standard pellet diet with free access and water *ad libitum*. Carbon tetrachloride, control and test compounds control administered orally which is briefed below.

Group-I (normal): rats were administered normal saline orally for 4 days.

Group-II (tacrine): rats administered tacrine orally 200 mg/kG daily for 4 days.

Group-III: rats received **6n** 200 mg/kg orally daily for 4 days.

Group-IV: rats were given **6o** 200 mg/kg orally daily for 4 days.

Group-V: rats received **6r** for four days 200 mg/kg orally daily.

Group-VI: rats administered orally CCl_4 2 ml/kg of 20% in olive nut oil single dose.

Blood samples were amassed on the fourth day and were subjected to centrifugation at 400 rpm for 15 min in order to separate the serum and refrigerated at −20 °C for further estimation of biomarkers for hepatotoxicity.

Biochemical analysis

Four biochemical markers levels from the serum which indicate the extent of hepatotoxicity viz. alanine amino transaminase (ALT), aspartate amino transaminase (AST), alkaline phosphatase (ALP) and total bilirubin levels were estimated spectroscopically by employing commercial kit from BioMed Diagnostics (White City, OR, USA).

Statistical analysis

Biochemical data were passed in to Prism GraphPad 8.0 for post experimental statistical analysis and results were expressed as mean ± SD. Two-way ANOVA followed by Tukey and Dunnet comparisons test was used to identify significance among groups. Statistical significance was accepted for values when $P < 0.05$.

Docking and molecular dynamics studies

Docking studies were carried out using Schrödinger software [29] (Version 2019-1, Schrödinger) (Glide module). The ligands used as inputs for docking were sketched by using ChemDraw software. Ligands were prepared using OPLS3e force field in Ligprep (Version 2019-1, Schrödinger). This minimization helps to assign bond orders and addition of the hydrogens to the ligands. The generated output file (Best conformation of the ligands) was used for docking studies. Protein was prepared by using the protein preparation in Maestro wizard [30] (Version 2019-1, Schrödinger). Hydrogen atom was added to the proteins and charges were assigned andalso generated Het states using epik at pH 7.2. Water molecules and other heteroatoms were excluded from the crystal structure as they were not significant for the

function of the protein in docking studies. Finally, the protein was optimized by using optimized potential liquid simulations (OPLS3) force field. A receptor grid was generated around the cocrystal ligand (X-ray pose of the ligand in the protein). The centroid of grid box and Vander Waal radius of receptor atoms was scaled to 1.00 Å with a partial atomic charge of 0.25. Glide docking score was used to determine the best docked structure from the output. Poses of the generated ligands after docking were analyzed by the help of XP Visualizer (Version 2019-1, Schrödinger).

Molecular dynamic studies were performed by using GROMACS 2019 [31] for esterase (PDB ID: 1EVE) in order to ascertain the stability of complex by applying CHARMM force field. Ligand topology was also generated by employing CHARMM General Force Field (CGenFF) [32]. Protein with **6o**ligand complex was solvated using predefined water model (TIP3P) [33] and complex was neutralized by addition of counter ions and subsequently minimized by following steepest descent method [34]. Entire system heated to 300 K for 100 ps timescale and followed by equilibration which was carried out in two different steps. First step, equilibration was conducted with constant volume and temperature and in second step, system was equilibrated with constant pressure and temperature. Finally, the complex was subjected to molecular dynamics for 6 ns and in order to evaluate the stability of structure, various parameters were evaluated, including RMSD, radius of gyration, RMSF and structural changes as a function of time.

Results and discussions

Chemistry

The synthesis of the target compounds **(6a-r)** has been accomplished in two steps as outlined in Scheme 1. A multicomponent reaction involving ethyl cyanoacetate**1**, aromatic aldehydes **2a-f**, 2-naphthol **3** and catalytic amount of piperidine in ethanol were refluxed at 80 °C for 6 hours to afford the respective ethyl 3-amino-1-phenyl-1H-benzo[*f*]chromene-2-carboxylates **4a-f** in good yield (52–64%). Further, ethyl 3-amino-1-phenyl-1H-benzo[*f*]chromene-2-carboxylate **4a-f** were refluxed with the appropriate commercial cycloketones **5a-c** in the presence of phosphorus oxytrichloride for 10 h to yield compounds13-phenyl-9,10,11,11a-tetrahydrobenzo[5,6]chromeno[*2,3-b*]cycloalkano[e] pyridin-12(13*H*)-ones **6a-r** in considerably low yields (32–45%). The physical characterization data of **6a-r** are listed in Table 1.

All the new compounds exhibited satisfactory spectral data correlating with their structures, FTIR spectrum of all final compounds **6a-r** showed carbonyl stretching vibration around 1704–1730 cm^{-1} and aliphatic CH stretching observed at the 2952–3090 cm^{-1}. The ^{1}H NMR data of the compounds

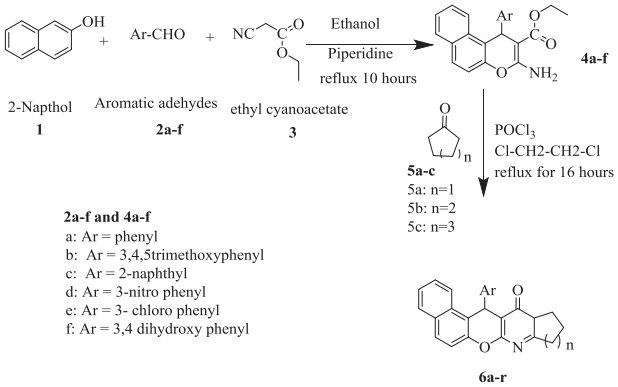

Scheme 1 Synthesis of 10,11,12,12a-tetrahydro-9H-benzo[5,6]chromeno[2,3-b]quinolin-13(14H)-one analogs

illustrated a multiplet at ~0.91–3.28 ppm assignable to saturated carbocyclic protons and aromatic protons resonated as multiplet in the range of 6.26–7.98 ppm. 3,4 dihydro-2H- pyran proton was found as a singlet in the range of 4.27–5.56. The ESI mass spectrometric data of all the compounds showed peaks at relevant $[M+H]^{+}$ m/z which complemented the FTIR and NMR spectra for the confirmation of expected structures of all the compounds.

Biochemical evaluation

In vitro AChE and BuChE inhibitory activity

All the 18 compounds have been screened against human AChE and BuChE by following reported methods and compared the potency with standards Tacrine and Donepezil. AChE and BuChE inhibitory activity can be tangibly correlated with structure of all compounds depending on the number of carbon atoms in saturated carbocyclic ring attached to the pyridine ring and substitution in the phenyl ring. AChE and BuChE inhibitory activities of all the compounds have been listed in Table 2 and graphically represented in Figs. 3 and 4.

Unsubstituted compound **6a** ($n=1$) with cyclopentano fused pyridine ring showed both AChE and BuChE with IC_{50} value of 2.1 and 6.16 µM. Most active compound among the series was found to be **6o** ($n=3$) with cycloheptane fused ring system with IC_{50} of 0.65 and 1.32 µM and compared to 0.47, 0.65 µM of tacrine and 0.71, 0.31 µM of donepezil against AChE and BuChE, respectively. In general, as the size of the carbocyclic ring increased the cholinesterase inhibitory activity was found to increase significantly. Among the unsubstituted compounds (**6p** and **6r**, Ar = Phenyl), as the size of carbocyclic ring increased from five to seven ($n=1$ to $n=3$), the potency against AChE was increased by about two times and more than three times increase in potency was observed against BuChE.

Table 1 Physical data of benzochromopyridones **6a-r**

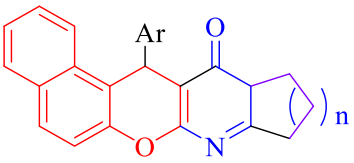

Comp.	n	Ar	M. Form	M. Wt	Rf[a]	% Yield
6a	1	Phenyl	$C_{25}H_{19}NO_2$	365	0.6	27
6b	2	Phenyl	$C_{26}H_{21}NO_2$	379	0.5	30
6c	3	Phenyl	$C_{27}H_{23}NO_2$	393	0.6	39
6d	1	2-Naphthyl	$C_{29}H_{21}NO_2$	415	0.4	26
6e	2	2-Naphthyl	$C_{30}H_{23}NO_2$	429	0.5	51
6 f	3	2-Naphthyl	$C_{31}H_{25}NO_2$	443	0.8	49
6 g	1	3-Chlorophenyl	$C_{25}H_{18}ClNO_2$	399	0.5	48
6 h	2	3-Chlorophenyl	$C_{26}H_{20}ClNO_2$	413	0.7	38
6i	3	3-Chlorophenyl	$C_{27}H_{22}ClNO_2$	427	0.5	45
6j	1	3-Nitro phenyl	$C_{25}H_{18}N_2O_4$	410	0.7	21
6k	2	3-Nitro phenyl	$C_{26}H_{20}N_2O_4$	424	0.5	40
6 l	3	3-Nitro phenyl	$C_{27}H_{22}N_2O_4$	438	0.6	36
6 m	1	3,4-Dihydroxyphenyl	$C_{25}H_{19}NO_4$	397	0.6	48
6n	2	3,4-Dihydroxyphenyl	$C_{26}H_{21}NO_4$	411	0.5	35
6o	3	3,4-Dihydroxyphenyl	$C_{27}H_{23}NO_4$	425	0.6	28
6p	1	3,4,5 Trimethoxy phenyl	$C_{28}H_{25}NO_5$	455	0.5	26
6q	2	3,4,5 Trimethoxy phenyl	$C_{29}H_{27}NO_5$	469	0.7	34
6r	3	3,4,5 Trimethoxy phenyl	$C_{30}H_{29}NO_5$	483	0.4	45

[a]Mobile phase: Hexane: ethyl acetate

Effect of the nature of aryl group and substituents on AChE and BuChE inhibitory activity was studied to understand the structure activity relationship. The simple phenyl group in **6a-c** (Ar = Ph) when replaced with naphthyl (**6d-f**, Ar = 2-naphthyl) resulted in marginal decrease in both cholinesterase inhibitory activities. This apparently hinted that large bulky substituent (Ar) could be detrimental for cholinesterase inhibitory activity. Substitution with 3-chloro group as in **6g-i** (Ar = 3-chlorophenyl) enhanced cholinesterase inhibitory activity significantly and compound **6i** with seven membered carbocyclic ring showed potent activity with IC_{50} value of 0.92 and 1.91 µM against AChE and BuChE, respectively.

Insertion of electron withdrawing group (2-nitro) as in **6j-l** resulted in decreased cholinesterase inhibitory activity when compared with their corresponding unsustituted compounds, **6a-c**, which indicated that electron withdrawing groups hinder the cholinesterase inhibitory activity. To explore further the SAR, compounds with two OH groups have been synthesized (**6m-o**) and to our expected observations, all the compounds were superior over **6a-c** and compound **6o** (Ar = 3,5-dihydroxyphenyl; $n = 3$) was found to be most potent among all the synthesized compounds with IC_{50} value of 0.65 and 1.32 µM against AChE and BuChE, respectively. Three compounds with 3,4,5-trimethoxyphenyl groups as in **6p-r** have also shown enhanced activity over unsubstituted compounds, **6a-c**, in both in vitro cholinesterase inhibitory activity.

In vitro brain AChE and BuChE inhibitory activity

Six potent compounds, **6 h, 6i, 6n, 6o, 6q and 6r**, were further tested for in vivo brain AChE and BuChE inhibitory activity along with tacrine and donepezil as standards by following the reported methodology. The in vivo brain AChE and BuChE inhibitory activities of tested compounds have been listed in Table 3 and depicted in Fig. 5.

Two chloro substituted compounds, **6h** ($n = 2$) and **6i** ($n = 3$), demonstrated potent brain AChE inhibitory activity with IC_{50} value of 44.14 and 30.35 µM, respectively, while dihydroxy compounds **6n** ($n = 2$) and **6o** ($n = 3$) showed potent AChE inhibitory activity with IC_{50} of 28.16 and 24.34 µM, respectively. Similarly, two trimethoxy substituted compounds **6q** and **6r** showed IC_{50} of 38.21 and 28.12 µM. In similar fashion to in vitro AChE and BuChE inhibitory activity as mentioned in the previous section, increase in the size of the enhanced the brain AChE inhibitory activity of synthesized compounds and compound **6o** proved to be the most potent in

Table 2 In vitro inhibitory activity of AChE/ BuChE of compounds **(6a-r)**

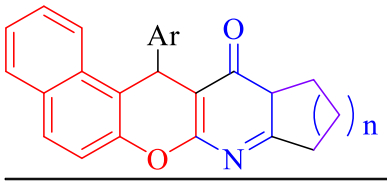

Comp.	n	Ar	AChE[a]	BuChE[a]	SI[b]
6a	1	Phenyl	2.10 ± 0.02	6.17 ± 0.02	2.84
6b	2	Phenyl	1.52 ± 0.04	5.02 ± 0.04	2.19
6c	3	Phenyl	1.12 ± 0.02	2.78 ± 0.04	2.77
6d	1	2-Naphthyl	2.35 ± 0.06	6.41 ± 0.03	1.67
6e	2	2-Naphthyl	1.80 ± 0.02	5.35 ± 0.03	3.0
6 f	3	2-Naphthyl	1.36 ± 0.03	4.26 ± 0.03	2.50
6 g	1	3-Chlorophenyl	1.35 ± 0.02	3.45 ± 0.03	2.46
6 h	2	3-Chlorophenyl	1.08 ± 0.03	2.38 ± 0.03	2.11
6i	**3**	3-Chlorophenyl	**0.92 ± 0.03**	**1.91 ± 0.02**	**2.07**
6j	1	3-Nitro phenyl	2.90 ± 0.02	7.64 ± 0.02	1.76
6k	2	3-Nitro phenyl	2.02 ± 0.04	5.59 ± 0.02	2.66
6 l	3	3-Nitro phenyl	1.65 ± 0.03	3.24 ± 0.03	1.98
6 m	1	3,4-Dihydroxyphenyl	1.91 ± 0.02	5.86 ± 0.03	1.84
6n	2	3,4-Dihydroxyphenyl	1.58 ± 0.03	4.15 ± 0.04	2.38
6o	**3**	3,4-Dihydroxyphenyl	**0.65 ± 0.06**	**1.32 ± 0.06**	**2.03**
6p	1	3,4,5 Trimethoxy phenyl	1.84 ± 0.05	5.14 ± 0.04	1.79
6q	2	3,4,5 Trimethoxy phenyl	1.26 ± 0.02	3.25 ± 0.02	2.42
6r	**3**	3,4,5 Trimethoxy phenyl	**0.85 ± 0.06**	**1.65 ± 0.06**	**1.94**
Tacrine	–		0.47 ± 0.02	0.65 ± 0.08	1.38
Donepezil	–		0.71 ± 0.06	0.31 ± 0.04	1.34

[a]IC_{50} Data are expressed as (mean ± SD) in µM, analyzed by one-way ANOVA followed by Tukey's multiple comparison test with $*p < 0.05$, $**p < 0.01$ as significant $n = 3$

[b]Selectivity index = IC_{50} (BuChE)/ IC_{50} (AChE)

inhibiting brain AChE and BuChE. However, in BuChE inhibitory activity, compound **6 h** ($n = 2$) was slightly better active than its seven membered analog **6i** ($n = 3$) and compound **6o** was also the most potent against BuChE with IC_{50} of 30.23 µM which was quite close to both tacrine and donepezil.

Behavioral studies

The statistical analysis was carried out by using Graphpad prism software version 5.0 and results were compared by one-way ANOVA followed by Tukey's Multiple Comparison Test. A $P \leq 0.001$ was considered as statistically significant.

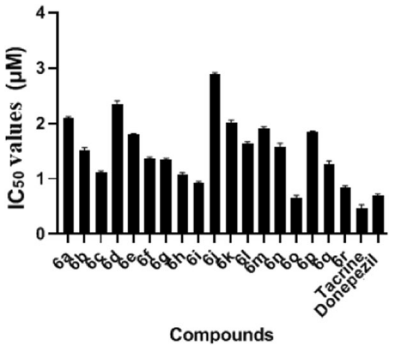

Fig. 3 AChE inhibitory activity (IC_{50} in µM) of compounds **6a-r**, tacrine and donepezil. The values represent the mean ± SD from three independent measurements

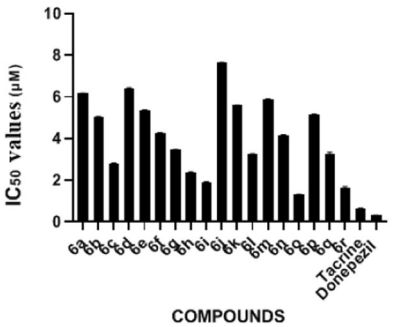

Fig. 4 BuChE inhibitory activity (IC_{50} in µM) of compounds **6a-r**, tacrine and donepezil. The values represent the mean ± SD (µM) from three independent measurements

Table 3 In vivo inhibitory activity of brain AChE/ BuChE of compounds **6 h, 6i, 6n, 6o, 6q** and **6r**

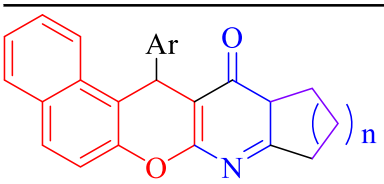

Group	AChE[a]	BuChE[a]
6 h	44.14 ± 0.18	35.10 ± 0.18
6i	30.35 ± 0.15	37.14 ± 0.24
6n	**28.16 ± 0.41**	**31.35 ± 0.17**
6o	**24.34 ± 0.24**	**30.23 ± 0.18**
6q	38.21 ± 0.20	40.35 ± 0.34
6r	28.12 ± 0.20	34.23 ± 0.51
Tacrine	18.10 ± 0.19	24.62 ± 0.32
Donepezil	20.20 ± 0.14	26.25 ± 0.25
Control	50.25 ± 0.52	55.20 ± 0.15

[a]IC_{50} Data are expressed as (mean ± SD) in µM, analyzed by one-way ANOVA followed by Tukey's multiple comparison test with $*p < 0.05$, $**p < 0.01$ as significant $n = 3$

Y maze model demonstrates a sensitive measure of spatial recognition memory in rodents. The result of the Y maze experiment is reported as % Alternations for both before and after the administration of test compounds (Table 4). All the test compounds and standards tacrine and donepezil have been administered with 400 mg/kg dose (p.o). The negative control group showed significant decrease in the Alternation when compared with the normal control. The results of the standards treated groups showed significant increase in the % Alternations with respect 6**i** and **6r** groups which are comparable with standard drug donepezil.

The learning scores (Transfer latency) obtained by each group in rectangular maze were suggestive of the fact that mice took lesser time on last day of study. Negative control group owed an increase in transfer latency score due to the memory deficit induced by β-amyloid peptide when compared to vehicle group. The transfer latency scores observed for the standard Tacrine treated animals are indicative of a significant ($P \leq 0.001$) memory enhancing potential compared to Negative control group. Similarly, groups treated with compounds **6i, 6 h** and **6r** afforded a significant reduction in transfer latency ($P \leq 0.001$) compared with the negative control group.

With the aim to assess avoidance behaviors, mice were subjected to conditioning tests in jumping box as this is reliable test for measuring the integrity of the learning and memory processes. Active avoidance behavioral responses, calculated as a cumulative number of shock avoidance during 15 trials in a day. In avoidance test, groups of animals administered with test compounds **6i** and **6r** showed significantly increased number of conditioned stimulus responses (avoidances) on the last day of study ($P \leq 0.001$) as compared with the negative control group animals. Animals treated with Tacrine and Donepezil showed significantly increased the number of conditioned stimulus responses (avoidances) on the last day of study ($P \leq 0.001$) as compared with the negative control group animals. While non-significant difference was observed between test group **6i** and **6r** as compared with these standard drugs signifies increase in the memory.

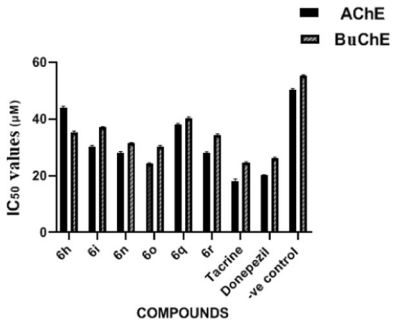

Fig. 5 Brain AChE and BuChE inhibitory activity (IC_{50} in μM) of compounds **6a-r**, tacrine and donepezil. The values represent the mean ± SD (μM) from three independent measurements

Hepatotoxicity studies

Three compounds **6n, 6o** and **6r** were subjected for assessing the serum ALP, ALT, AST and total bilirubin levels, which indicate the extent of hepatotoxicity caused by the test compounds and are compared with tacrine as standard in carbon tetrachloride induced hepatotoxicity test protocol. The serum biomarkers' data of test compounds, standard and control groups has been listed in Table 5. Tacrine has been included in the study as standard due its high hepatotoxicity due to which tacrine has been discontinued from the market. Single dose of CCl_4 has resulted in drastic 3 to 4 fold increase in serum biomarkers' levels when compared with normal saline administered control group. The tacrine treated group also

Table 4 Effect on biochemical parameters of liver function tests

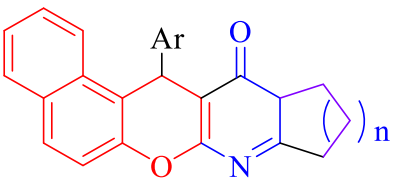

Groups	Bilirubin	ALP*	ALT*	AST[a]
6n	24.96 ± 1.68	82.43 ± 2.25	51.43 ± 0.86	133.6 ± 3.14
6o	21.63 ± 1.42	75.0 ± 3.26	45.33 ± 1.75	124.83 ± 1.59
6r	26.76 ± 1.19	94.53 ± 1.75	63.73 ± 1.43	150.63 ± 7.90
Tacrine	64.56 ± 3.95	117.86 ± 4.80	82.33 ± 1.10	198.2 ± 7.51
Control	21.03 ± 1.64	85.93 ± 1.82	41.06 ± 1.47	123.53 ± 2.75
CCl_4 group	117.5 ± 7.25	261.16 ± 7.13	133.06 ± 3.66	395.16 ± 10.30

[a]Data expressed in U/L, as (mean ± SD) $n = 6$ animals in each group analyzed by one-way ANOVA followed by Tukey's multiple comparison test with $^{***}p < 0.001$ as significant

Table 5 Behavioral effects in Y-maze, rectangular maze and jumping box tests

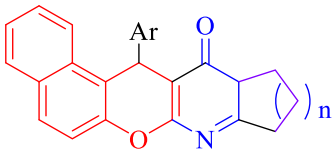

Comp	Y-maze test (% Alternations)		Rectangular maze (sec)		Jumping box (sec)	
	Before treatment	After treatment	Before treatment	After treatment	Before treatment	After treatment
6a	22.15 ± 1.25	32.13 ± 1.08	149.63 ± 2.20	134.45 ± 2.35	30.10 ± 2.45	21.01 ± 2.45
6b	20.15 ± 1.56	33.84 ± 1.65	148.26 ± 1.23	130.01 ± 2.40	31.23 ± 2.54	19.43 ± 2.54
6c	21.15 ± 1.38	35.12 ± 1.46	151.16 ± 1.86	124.32 ± 1.48	30.15 ± 2.10	17.56 ± 2.10
6d	20.32 ± 1.03	31.20 ± 2.14	150.18 ± 1.24	138.12 ± 1.24	31.6 ± 3.56	22.15 ± 2.56
6e	25.62 ± 1.30	32.32 ± 1.87	149.28 ± 1.35	136.20 ± 2.35	26.15 ± 2.45	18.08 ± 1.45
6 f	21.30 ± 1.30	34.24 ± 3.14	148.28 ± 1.40	130.18 ± 2.40	28.18 ± 2.54	16.12 ± 1.54
6 g	22.02 ± 1.38	42.13 ± 1.87	151.12 ± 3.40	104.15 ± 1.40	30.23 ± 2.54	14.12 ± 2.54
6 h	20.10 ± 2.25	46.14 ± 2.65	152.72 ± 2.37	98.75 ± 2.37	29.05 ± 1.23	12.17 ± 1.23
6i	**23.42 ± 1.03**	**50.61 ± 1.87**	**150.15 ± 1.85**	**90.15 ± 1.82**	**32.6 ± 1.62**	**10.24 ± 1.62**
6j	20.12 ± 1.25	30.20 ± 2.10	149.21 ± 1.98	132.07 ± 2.35	26.20 ± 2.15	20.43 ± 2.15
6k	22.20 ± 1.00	31.15 ± 1.50	150.14 ± 2.48	129.07 ± 1.32	34.10 ± 3.18	18.42 ± 3.18
6 l	21.27 ± 1.02	32.65 ± 1.46	150.76 ± 1.37	126.75 ± 1.37	29.5 ± 0.22	16.17 ± 0.22
6 m	20.35 ± 1.12	37.61 ± 3.15	151.12 ± 2.40	120.15 ± 1.40	30.23 ± 1.54	16.12 ± 1.20
6n	21.22 ± 1.29	39.12 ± 1.46	148.28 ± 1.87	116.18 ± 1.25	28.18 ± 2.54	14.16 ± 1.54
6o	22.14 ± 1.32	42.12 ± 2.58	149.24 ± 1.35	110.07 ± 2.35	30.20 ± 2.45	12.45 ± 2.45
6p	20.23 ± 1.23	36.15 ± 1.23	150.28 ± 2.07	125.30 ± 1.07	30.16 ± 1.65	17.23 ± 1.25
6q	21.05 ± 1.35	38.35 ± 1.35	151.23 ± 1.65	120.10 ± 1.25	31.40 ± 1.65	14.13 ± 2.35
6r	**20.12 ± 1.03**	**48.25 ± 1.46**	**150.18 ± 1.42**	**102.24 ± 2.65**	**30.18 ± 1.20**	**12.33 ± 1.20**
Tacrine	**20.60 ± 1.18**	**54.32 ± 2.06**	**150.42 ± 2.21**	**78.61 ± 2.21**	**28.32 ± 0.71**	**8.30 ± 0.71**
Donepezil	21.28 ± 2.42	48.32 ± 2.58	151.42 ± 1.21	92.61 ± 2.21	28.32 ± 0.71	9.30 ± 0.71
-ve	23.19 ± 2.18	142.87 ± 2.53	34.12 ± 1.09			
Vehicle control	47.61 ± 3.15	47.83 ± 2.53	12.5 ± 2.18			

demonstrated trend of increase in the levels of biomarkers; however, levels were not high as of CCl_4 treated group. All the three test compounds have shown bilirubin level on par with control group and compound **6r** exhibited slightly elevated ALP level where as **6n** and **6o** treated groups have ALP level slightly lesser than control group. ALT and AST levels of **6r** treated group were found to be higher than control group while compounds **6n** and **6o** treated groups showed similar profile as of control group. The aforementioned data on levels of four biomarkers and bilirubin revealed that synthesized compounds are devoid of hepatotoxicity unlike the standard tacrine Fig. 6.

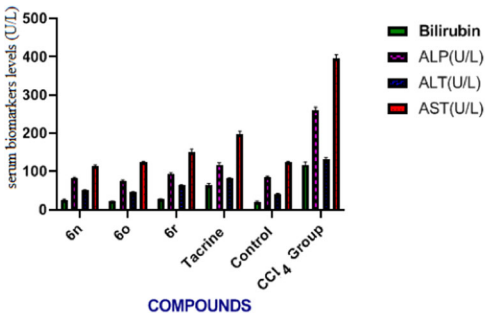

Fig. 6 Effect of test compounds, tacrine, on CCl_4 induced serum levels of Bilirubin, ALP, ALT and AST. The values represent the mean ± SD from three independent measurements

Docking and molecular dynamics studies

In vitro studies of synthesized compounds showed the potential cholinesterase inhibitory activity and among all, the compound **6r** showed promising cholinesterase inhibitory activity. These result encouraged us to perform docking studies to get the insight in to the binding mode of synthesized compounds within binding pocket of AChE and BChE. All structures of ligands were built using maestro and further prepared using LigPrep form Schrodinger package. Protein

structures were obtained from the Protein Data Bank (PDB ID: acetyl cholinesterase-1EVE and butylcholinesterase-4BDS) and necessary correction to the protein structure were done using Protein Preparation Wizard in Schrodinger package. Docking studies were performed using Glide docking software and docking protocol was validated by docking the cocrystal ligand which resulted with RMSD of docked conformation and cocrystal ligand pose was found to be 0.6. The binding interactions of compounds with AChE and BChE have been listed in Tables 6 and 7.

Docking study was performed on the both R and S enantiomers of all compounds, among both conformations, R enantiomers were better in demonstrating docking interactions. Binding poses of synthesized compounds with AChE have shown that these molecules bind well within binding pocket of enzyme. Among the all synthesized molecules, **6r** with potent cholinesterase inhibitory activity, has shown the highest binding score. In superimposed pose of **6r** with cocrystal ligand, pentacycline ring was coinciding with skeleton of cocrystal ligand as depicted in Fig. 7. However, 3,4,5-triimethoxyphenyl ring has occupied the empty additional space available in binding pocket. In binding pocket, **6r**was involved in π-π stacking interactions with Phe331 and His440. 3-methoxy group formed hydrogen bond with side chain of Ser122 while 4-methoxy group was involved in hydrogen

Table 6 Docking energies of 6a-r in AChE and BuChE

Comp.	Docking score AChE	Docking score BChE
Cocrystal Ligand	−8.633	−6.015
6r-R	−11.85	−8.803
6p-R	−10.666	−8.213
6m-R	−10.579	−8.185
6q-R	−10.529	−7.78
6o-R	−9.607	−7.408
6f-R	−9.5	−7.388
6d-R	−8.88	−7.311
6n-R	−8.584	−7.046
6l-R	−8.381	−6.981
6e-R	−8.36	−6.914
6g-R	−8.278	−6.894
6k-S	−8.049	−6.799
6j-S	−7.759	−6.68
6c-S	−6.262	−6.517
6b-S	−6.195	−6.483
6a-S	−6.194	−6.098
6i-S	−6.046	−5.775
6h-R	−5.595	−5.417

Table 7 Analysis of Amino-acid residues participated in the interactions with the proteins (4BDS, 1EVE)

PDB 4BDS	H-bond Interactions	Aromatic bond Interactions	pi–pi Interactions
6q	SER198	HIS438, ALA328	–
6n	–	PHE329	ALA328
6 h	–	ASP70, TRP82 ASN83, PHE329	–
Crystal ligand	HIS438	HIS438	TRP82
PDB 1EVE	**H-bond Interactions**	**Aromatic bond Interactions**	**pi-pi Interactions**
6q	–	–	TRP-279
6n	SER122	ASP72, PHE331 GLU199	TYR121, TYR334 HIS440, PHE331
6 h	–	ASP72, GLU199	TYR121, PHE331 HIS440
Crystal ligand	–	TYR130, PHE331	–

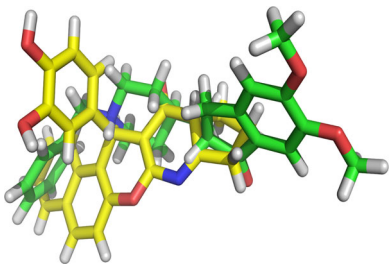

Fig. 7 Superimposed pose of **6r** (yellow) with co-crystal ligand (green)

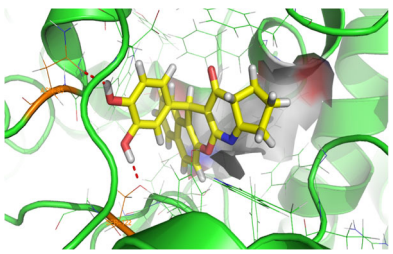

Fig. 8 Docking pose of **6r** (yellow) with AChE (green) where hydrogen bonds are shown in red dotted line

bonding with side chain carbonyl carbon of Asn80 (Fig. 8). Cyclopentane ring was found to involve in hydrophobic contacts with Tyr334 and Phe331 and Naphthalene ring was in close proximity with Trp84, Glu199, His440 and Gly441. Moreover, docking studies on the BuChE showed the similar results as acetylcholinesterase. Compound **6r** has the highest binding score and 3,4,5-trimethoxyphenyl was involved in hydrogen bonding interactions with enzyme; 3-methoxy group with His148, whereas 4-methoxy was forming with Gly78 and Trp82 (Fig. 9).

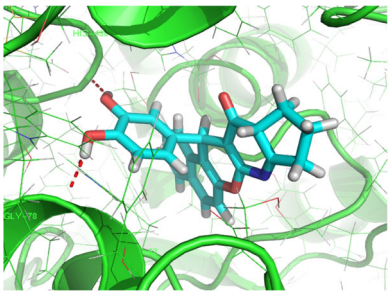

Fig. 9 Docking pose of **6r** (cyan) with BChE (green) where hydrogen bonds are shown in red dotted line

Molecular dynamics study was performed on the protein complex with ligand **6o** to explore the stability of complex based on data garnered on RMSD, Rg, RMSF, pre and post molecular dynamics structure analysis as a function of time. RMSD of backbone atoms was found around 0.2 nm which supports the stability of the structure (Fig. 10a) and RMSD for ligand heavy atoms settled in the range of 0.06 nm (Fig. 10b) and also the integrity was maintained throughout the simulation. Flexible and rigid regions were analyzed using RMSF which revealed the stability of the complex (Fig. 10c), except for the terminal residues. Radius of gyration was observed around 2.3 nm which indicates the tight compactness of the protein ligand complex (Fig. 10d). Moreover, the comparison of the pre and post molecular dynamics structure shown that there are no substantial changes in the structure (Fig. 11) with RMSD of 1.282 which also hinted that the complex was stable.

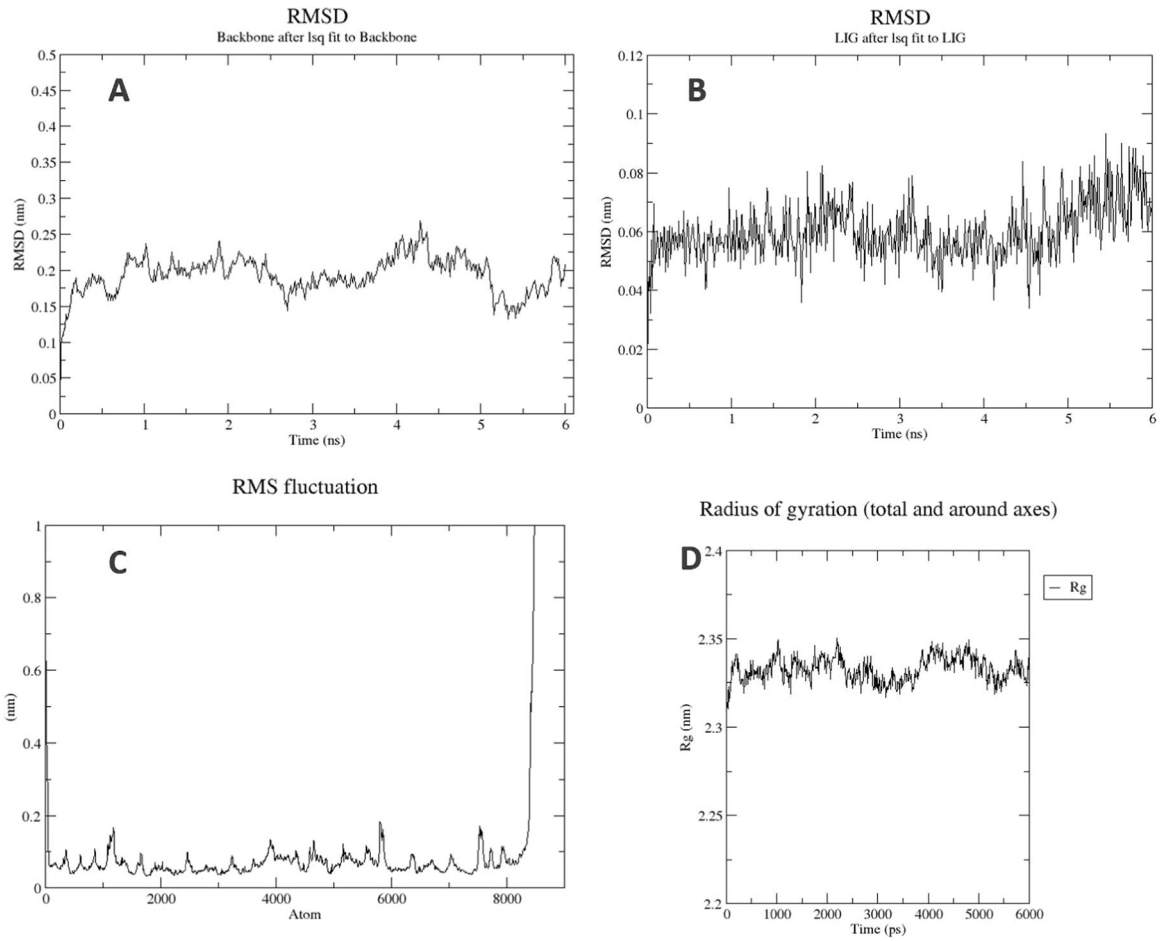

Fig. 10 Molecular dynamics analysis for esterase. **a** RMSD for protein backbone, **b** RMSD for the ligand, **c** RMSF for protein and ligand and **d** radius of gyration

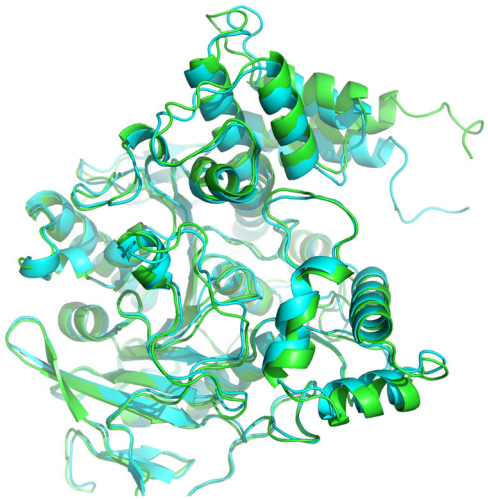

Fig. 11 Pre (green) and post (cyan) molecular dynamics structure of esterase

Conclusions

In a multicomponent reaction and subsequent Friedlander reaction to yield *10,11,12,12a-tetrahydro-9H-benzo[5,6]chromeno[2,3-b]quinolin-13(14H)-ones* **(6a-r)** were aimed for the inhibition of both AChE and BuChE, which are the attractive targets for developing new potent molecules useful in the treatment of AD. All the synthesized compounds showed activity in micromolar and submicromolar levels against AChE and BuChE. Most potent cholinesterase inhibitory activity exhibited by compound bearing 3,5-dihydroxy phenyl group at 15th position of hexahydrobenzo [5,6]chromeno[2,3-b] cyclohepta[e]pyridin-14(15*H*)-one scaffold, **6o**, with IC_{50} of 0.65 µM against AChE and 1.32 µM against BuChE. Apart from **6o**, a trimethoxy phenyl derivative **6r** exhibited demonstrated IC_{50} of 0.85 and 1.65 µM selectively against AChE and BChE, respectively. Size of the cycloalkane ring influenced toward the potency. Along with selective cholinesterase inhibitory activity, both **6o** and **6r** were safe in hepatotoxicity when compared to tacrine which is known for hepatotoxicity. Both **6o** and **6r** were equally active in behavioral studies involving Y maze, rectangle maze and jumping box test comparable with standard drug tacrine. **6r** emerged with topmost binding score in docking studies which depicted the trimethoxy phenyl group occupied additional void hydrophobic area. Contemplation of the compounds **6a-r** obtained in good yields, potent in vitro AChE and BuChE inhibitory activity, lower hepatotoxicity along with encouraging CNS behavioral activities make them one of the new lead molecules in the development of drugs for the treatment of AD.

Acknowledgements One of the authors BM expresses thank to the University Grants Commission, New Delhi for financial support of this study. Authors thank the Principal, University College of Pharmaceutical Sciences, Kakatiya University, Warangal for providing necessary facilities. Authors RK and CB express gratitude Mr. Raghu Rangaswami and Dr. Prajwal Nandekar, Schrodinger, Bangalore for granting free one-monthlicense of Schrodinger Suite 2019 for docking studies. Both RK and CB appreciate the Principal and Management of Bharati Vidyapeeth's Poona College of Pharmacy, Pune for providing all computational facilities.

Compliance with ethical standards

Conflict of interest The authors declare that they have no conflict of interest.

Publisher's note Springer Nature remains neutral with regard to jurisdictional claims in published maps and institutional affiliations.

References

1. Goedert M, Spillantini MG. A century of Alzheimer's disease. Science. 2006;314:777–81. https://doi.org/10.1126/science.1132814
2. Wimo A, Prince M, Guerchet M, Ali GC, Wu YT, Prina M. World Alzheimer Report 2015. 2015. http://www.alz.co.uk/worldreport
3. Andreeva T, Lukiw WJ, Rogaev EI. Biological basis for Amyloidogenesis in Alzheimer's disease. Biochem. (Moscow). 2017;82:122–39. https://doi.org/10.1134/s0006297917020043
4. Jucker M, Walker LC. Pathogenic protein seeding in Alzheimer's disease and other neurodegenerative disorders. Annal Neuro. 2011;70:532–40. https://doi.org/10.1002/ana.22615
5. Sultana R, Butterfield DA. Role of oxidative stress in the progression of Alzheimer's disease. J Alzheimer's Dis. 2010;19:341–53. https://doi.org/10.3233/jad-2010-1222
6. Kaur R, Mehan S, Singh S. Understanding multifactorial architecture of Parkinson's disease: pathophysiology to management. Neurological Sci. 2019;40:13–23. https://doi.org/10.1007/s10072-018-3585-x
7. Meng Q, Ru J, Zhang GL. Re-evaluation of tacrine hepatotoxicity using gel entrapped hepatocytes. Toxicol Lett. 2007;168:140–7. https://doi.org/10.1016/j.toxlet.2006.11.009
8. Wu WY, Chendai YU, Gu T. Novel multitarget-directed tacrine derivatives as potential candidates for the treatment of Alzheimer's disease. J Enzyme Inhib Med Chem. 2017;32:572–87. https://doi.org/10.1080/14756366.2016.1210139
9. Cavalli A, Bolognesi ML, Minarini A. Multi-target-directed ligands to combat neurodegenerative diseases. J Med Chem. 2008;51:347–72. https://doi.org/10.1021/jm7009364
10. Chen X, Decker ME. Multi-target compounds acting in the central nervous system designed from natural products. Cur Med Chem. 2013;20:1673–85. https://doi.org/10.2174/0929867311320130007
11. Wang Y, Wang F, Yu JP. Novel multipotent phenylthiazole-tacrine hybrids for the inhibition of cholinesterase activity, β-Amyloid aggregation and Ca^{2+} overload. Bioorg Med Chem. 2012;20:6513–522. https://doi.org/10.1016/j.bmc.2012.08.040
12. Mohamed T, Rao PP. Alzheimer's disease: emerging trends in small molecule therapies. Cur Med Chem. 2011;18:4299–320. https://doi.org/10.2174/092986711797200435
13. Eghtedari M, Sarrafi Y, Nadri H, Mahdavi M, Moradi A, Homayouni MF, et al. New tacrine-derived AChE/BuChE inhibitors: Synthesis and biological evaluation of 5-amino-2-phenyl-4H-pyrano[2,3-b]quinoline-3-carboxylates. Eur J Med Chem. 2017;128:237–46. https://doi.org/10.1016/j.ejmech.2017.01.042
14. Pourabdi L, Khoobi M, Nadri H, Moradi A, Moghadam F, Emami S, et al. Synthesis and structure activity relationship study of

tacrine-based pyrano[2,3-c] pyrazole stargeting AChE/BuChE and 15-LOX. Eur J Med Chem. 2016;123:298–308. https://doi.org/10.1016/j.ejmech.2016.07.043
15. Maalej E, Chabchoub F, Oset-Gasque MJ, Samadi MJ. Synthesis, biological assessment, and molecular modeling of racemic 7-aryl-9,10,11,12-tetrahydro-7H-benzo [7,8] chromeno[2,3-b]quinolin-8-amines as potential drugs for the treatment of Alzheimer's disease. Eur J MedChem. 2012;54:750–63. https://doi.org/10.1016/j.ejmech.2012.06.038
16. Dgachi Y, Bautista OM, Benchekroun M, Martin H, Bonet A, Marco-Contelles J, et al. Synthesis and biological evaluation of benzochromenopyrimidinones as cholinesterase inhibitors and potent antioxidant, non-hepatotoxic agents for Alzheimer's disease. Mol. 2016;21:634. https://doi.org/10.3390/molecules21050634
17. Hanish Singh JC, Alagarasamy V, Diwan PV, Kumar SS, Nisha JS, Reddy YN. Neuroprotective effect of Alpiniagalanga (L) fractions on Aβ(25-35) induced amnesia in mice. J Ethno Pharmacol. 2011;138:85–91. https://doi.org/10.1016/j.jep.2011.08.048
18. Almoazen H, Bhattacharjee H, Samse AC, Patel S. Stability of mesna in readymade infusion devices. Ann Pharmacother. 2010;44:224–5. https://doi.org/10.1345/2Faph.1M390
19. Ellman GL, Courtney KD, Anders V, Featherstone RM. New and rapid colorimetric determination of acetyl cholinesterase activity. Biochem Pharmacol. 1961;7:88–95. https://doi.org/10.1016/0006-2952(61)90145-9
20. Barros DM, Izquierdo LA, Mello ST, Ardenghi P, Pereira P, Medina JH, et al. Molecular signaling pathways in the cerebral cortex are required for retrieval of one-trial inhibitory avoidance learning in rats. Behav Brain Res. 2000;114:183–92. https://doi.org/10.1016/S0166-4328(00)00226-6
21. Bornschein RL, Hastings L, Manson JM. Behavioral toxicity in the offspring of rats following maternal exposure to dichloromethane. Toxic Appl Pharmacol. 1980;52:29–37. https://doi.org/10.1016/0041-008X(80)90244-6
22. Garofalo P, Colombo S, Lanza M, Revel L, Makovec F. New putative memory enhancer, behavioral studies on learning and memory in rats and mice. J Pharm Pharmacol. 1996;48:1290–7. https://doi.org/10.1111/j.2042-7158.1996.tb03938.x
23. Buresova O, Bures J, Oitzl MSA. Radial maze in the water tank: an aversively motivated spatial working memory task Zahalka. Physiol Behav. 1985;34:1003–5. https://doi.org/10.1016/0031-9384(85)90028-9
24. Shear DA, Dong J, Creguer KL, Bazzett TJ, Albin RL, Dunbar GL. Chronic administration of quinolinic acid in the rat striatum causes spatial learning deficits in a radial arm water maze task. Exp Neurol. 1998;150:305–11. https://doi.org/10.1006/exnr.1998.6767
25. Goodarzi Z, Mele B, Guo S, Hanson H, Jette N, Patten S, et al. Guidelines for dementia or Parkinson's disease with depression or anxiety, a systematic review. BMC Neurol. 2016;16:244–8. https://doi.org/10.1186/s12883-016-0754-5
26. Conrad CD, Lupien SJ, Thanasoulis LC, McEwen BS. The effects of type I and type II corticosteroid receptor agonists on exploratory behavior and spatial memory in the Y-maze. Brain Res. 1997;759:76–83. https://doi.org/10.1016/S0006-8993(97)00236-9
27. Letteron P, Labbe G, Degott C, Berson A, Fromenty B, Larrey M, et al. Mechanism for the protective effects of silymarin against carbon tetrachloride-induced lipid peroxidation and hepatotoxicity in mice, evidence that silymarin acts both as an inhibitor of metabolic activation and as a chain-breaking antioxidant. Bio Chem Pharmacol. 1990;39:2027–34. https://doi.org/10.1016/0006-2952(90)90625-u
28. Tsai JH, Liu JY, Wu TT, Ho PC, Huang CY, Shyu JC, et al. Effects of silymarin on the resolution of liver fibrosis induced by carbon tetrachloride in rats. J Viral Hep. 2008;15:508–14. https://doi.org/10.1111/j.1365-2893.2008.00971x
29. Schrödinger Release 2019-1: Schrödinger Suite 2019-1 Protein Preparation Wizard; Epik, Schrödinger, LLC, New York, NY, 2019
30. Dizdaroglu Y, Albay C, Arslan T, Ece A, Emir A, Turkoglu E, et al. Design, synthesis and molecular modelling studies of some pyrazole derivatives as carbonic anhydrase inhibitors. J Enzyme Inhib Med Chem. 2020;35:289–97. https://doi.org/10.1080/14756366.2019.1695791
31. Van Der Spoel D, Lindahl E, Hess B, Groenhof G, Mark AE, Berendsen HJ. GROMACS: fast, flexible, and free. J Comput Chem. 2005;26:1701–18. https://doi.org/10.1002/jcc.20291
32. Vanommeslaeghe K, Hatcher E, Acharya C, Kundu S, Zhong S, Shim J, et al. CHARMM general force field: A force field for drug-like molecules compatible with the CHARMM all-atom additive biological force fields. J Comp Chem. 2010;31:671–90. https://doi.org/10.1002/jcc.21367
33. Vanommeslaeghe K, MacKerell AD Jr. Automation of the CHARMM General Force Field (CGenFF) I: bond perception and atom typing. J Chem Inf Model. 2012;52:3144–54. https://doi.org/10.1021/ci300363c
34. Bjelkmar P, Larsson P, Cuendet MA, Hess B, Lindahl E. Implementation of the CHARMM force field in GROMACS: analysis of protein stability effects from correction maps, virtual interaction sites, and water models. J Chem Theory Comp. 2010;6:459–66. https://doi.org/10.1021/ct900549r